



Differential roles of the frontal and parietal cortices in the control of saccades



Julia Bender^{a,*}, Kyeong-Jin Tark^b, Benedikt Reuter^a, Norbert Kathmann^a, Clayton E. Curtis^{b,c}

^a Department of Psychology, Humboldt-Universität zu Berlin, Germany

^b Department of Psychology, New York University, New York, NY, USA

^c Center for Neural Science, New York University, New York, NY, USA

ARTICLE INFO

Article history:

Accepted 17 June 2013

Available online 15 July 2013

Keywords:

Action control

fMRI

MVPA

Saccades

Volition

ABSTRACT

Although externally as well as internally-guided eye movements allow us to flexibly explore the visual environment, their differential neural mechanisms remain elusive. A better understanding of these neural mechanisms will help us to understand the control of action and to elucidate the nature of cognitive deficits in certain psychiatric populations (e.g. schizophrenia) that show increased latencies in volitional but not visually-guided saccades. Both the superior precentral sulcus (sPCS) and the intraparietal sulcus (IPS) are implicated in the control of eye movements. However, it remains unknown what differential contributions the two areas make to the programming of visually-guided and internally-guided saccades. In this study we tested the hypotheses that sPCS and IPS distinctly encode internally-guided saccades and visually-guided saccades. We scanned subjects with fMRI while they generated visually-guided and internally-guided delayed saccades. We used multi-voxel pattern analysis to test whether patterns of cue related, preparatory and saccade related activation could be used to predict the direction of the planned eye movement. Results indicate that patterns in the human sPCS predicted internally-guided saccades but not visually-guided saccades in all trial periods and patterns in the IPS predicted internally-guided saccades and visually-guided saccades equally well. The results support the hypothesis that the human sPCS and IPS make distinct contributions to the control of volitional eye movements.

© 2013 Elsevier Inc. All rights reserved.

1. Introduction

Experimental eye movement tasks have been used widely to investigate mechanisms of action control in primates. Importantly, eye movement tasks allow the useful comparison of top-down self-initiated action with bottom up stimulus-driven behavior that has identical motor parameters (Reuter & Kathmann, 2004). Stimulus-driven behavior is required in visually-guided saccade tasks where a visual signal (exogenous cue) is directly transformed into a motor signal with identical spatial coordinates (Munoz & Everling, 2004). Saccade generation is therefore largely controlled by the visual stimulus. In contrast, simple internally-guided saccades require a gaze shift towards a location that is indicated by an arbitrary cue (e.g. a tone or central endogenous cue). Here, the gaze shift is based on the internal representation of a task rule (e.g. arrow or symbol indicates saccade direction). Since there are no other cognitive requirements, differences between simple internally-guided saccades and visually-guided saccades with identical motor demands can be attributed to differences in the demands on volitional con-

trol. Notably, psychiatric populations such as schizophrenia patients show longer latencies in simple internally-guided tasks, suggesting a circumscribed deficit in volitional saccade generation (Reuter & Kathmann, 2007). Understanding the nature of the difference between visually-guided saccades and simple internally-guided saccades therefore seems highly relevant to understand basic mechanisms of volitional action control and key symptoms of common psychiatric disorders.

Studies comparing simple internally-guided saccades with visually-guided saccades are relatively rare. These studies found increased latencies in simple internally-guided saccades compared to visually-guided saccades (Mort et al., 2003; Reuter, Kaufmann, Bender, & Kathmann, 2010; Walker, Walker, Husain, & Kennard, 2000). Using functional magnetic resonance imaging (fMRI) Mort et al. (2003) compared simple internally-guided saccades and visually-guided saccades and found relatively increased activation for internally-guided saccades in the intraparietal sulcus (IPS) and in the putative human homologue of the monkey frontal eye field (FEF), which is thought to reside in the superior precentral sulcus (sPCS) at its junction with the superior frontal sulcus (Mort et al., 2003). However, other studies found the reversed pattern with higher activation in the sPCS and IPS for visually-guided saccades compared to internally-guided saccades (Schraa-Tam et al., 2009)

* Corresponding author. Address: Department of Psychology, Clinical Psychology, Rudower Chaussee 18, 12489 Berlin, Germany. Fax: +49 (0)30 2093 4859.

E-mail address: benderjx@hu-berlin.de (J. Bender).

or no difference in brain activation between the tasks (Reuter et al., 2010).

Most studies investigating the differences in stimulus driven and more volitional eye movements have relied on more complex eye movement tasks such as the antisaccade task (Hallett, 1978; Hutton & Ettinger, 2006) and the oculomotor delayed response (ODR) task (Hikosaka & Wurtz, 1983). In the ODR task subjects have to remember the location of a visual target throughout a delay, and make a memory-guided saccade after the delay. A common finding is that latencies are longer for complex internally-guided saccades than for visually-guided saccades (Hutton, 2008). Furthermore, the sPCS, the IPS, the supramarginal gyrus and the dorsolateral prefrontal cortex (DLPFC) show sustained activation during the retention interval of memory-guided saccade tasks (Curtis & D'Esposito, 2006; Curtis, Rao, & D'Esposito, 2004). It has been argued that the activity in the sPCS reflects the coding of the location of the cue and the saccade (Geier, Garver, & Luna, 2007; Srimal & Curtis, 2008). Single cell recordings in monkeys suggest that IPS activation during the delay codes the location of the upcoming saccade (Mazzoni, Bracewell, Barash, & Andersen, 1996). Notably, the oculomotor delayed response task requires additional cognitive processes beyond the memory-guided saccade. The longer latencies and differences in brain activation found for these complex internally-guided saccades in comparison to visually-guided saccades might reflect the inhibition of anticipatory responses, spatial working memory or programming an internally-guided saccade (Hutton, 2008; Walker et al., 2000).

Taken together, previous studies suggest that frontoparietal regions, especially the sPCS and the IPS play a crucial role in the volitional generation of saccades. However, the unique contributions of each area and the specific mechanisms used for generating volitional saccades remain unclear. As described above, the findings from brain imaging studies are inconsistent when comparing simple internally-guided saccades to visually-guided saccades and suggest that such univariate comparisons only evokes subtle differences, if any, in the relative amount of brain activity. A new and effective method of analyzing functional brain imaging data is multivoxel pattern analysis (MVPA). In contrast to traditional (univariate) approaches that analyze the time course of each voxel independently, MVPA uses small differences in the fMRI response between voxels to estimate different brain states. Between voxel differences are assumed to reflect subtle biases in the spatial distribution of the neural subpopulations sampled by each voxel. There is growing evidence that such multivariate techniques can distinguish between responses to different stimuli where more traditional, voxel-wise univariate approaches, or signal averaging across whole regions of interest could not (Haynes & Rees, 2006; Kriegeskorte, 2011; Kriegeskorte & Bandettini, 2007; Pereira, Mitchell, & Botvinick, 2009).

In the present fMRI study, besides conventional whole brain and region of interest analyses we used MVPA to find differences in neural activation in sPCS and IPS during the performance of visually-guided and volitional, internally-guided saccades. Since the MVPA method benefits from data acquired in a blocked design, whereas an event-related design is optimal for adaptation methods we optimized our paradigm for both methods. We used visually-guided saccades and internally-guided saccades in an oculomotor delayed response paradigm that allowed event related modeling of the trials of each condition and the acquisition of sufficient blocked timepoints for the MVPA analysis during the delay. As described above, the oculomotor delayed response paradigm presumably demands inhibition of anticipatory responses and spatial working memory, since the saccade has to be postponed until the end of the delay. However, in the present study inhibition and working memory demands were held equal for both task conditions so that differences could be ascribed to the differences in

the nature of the exogenous or endogenous instruction. Our special interest therefore lay on the cue and delay period when the visually-guided and internally-guided instruction was encoded and transcribed into a motor plan.

2. Methods

2.1. Participants

13 Neurologically healthy subjects were recruited (7 females, mean age 28.08 years, range 20–40 years). All subjects gave written informed consent according to procedures approved by the human subjects Institutional Review Board at New York University.

2.2. Task design

All stimuli were presented on a gray background. Throughout the experiment two white circular placeholders (diameter, 1° of visual angle) were visible on the screen at 5° of visual angle left and right of the center of the screen. Subjects performed saccades in two conditions of the delayed saccade task paradigm. Trials were organized in three trial periods: cue, delay and response. Each trial began with a fixed fixation interval (1.75 s) where subjects fixated a white cross at the center of the screen.

In the delayed internally-guided saccade condition, thought to depend on volitional control, a white arrow head (cue) pointing left or right was flashed for 180 ms at the center of the screen where the fixation cross had been. After the presentation of the endogenous cue the fixation cross reappeared at the center and the delay began. Subjects were instructed not to make a saccade right away but to prepare a saccade towards the placeholder indicated by the arrowhead. During the fixed length delay period (8.57 s) the fixation cross and the placeholders were displayed on the screen to facilitate preparation (Fischer et al., 1993). After the delay the fixation cross disappeared, instructing subjects to make a saccade to the indicated placeholder (leftward or rightward saccade). The saccade response period lasted for 1.75 s and was followed by a randomized inter-trial interval of 7–12.25 s in which only the fixation cross was present and subjects maintained fixation at the center of the screen.

The delayed visually-guided saccade condition, thought to depend less on volitional control, only differed from the delayed internally-guided saccade condition with respect to the cue. After the initial fixation interval the fixation cross remained visible at the center and a white dot (exogenous cue) appeared in either the left or right placeholder for 180 ms. Subjects were instructed not to make a saccade right away but to prepare a saccade towards the indicated placeholder (left or right) and to execute the saccade when the fixation cross disappeared after the delay.

Trials were presented in six blocks with both conditions pseudo-randomly mixed. Two subjects only performed five blocks due to technical problems. Each block consisted of 24 trials. To keep alertness high, four of the 24 trials were catch trials that ended after the presentation of the cue. Catch trials were not analyzed. Fig. 1 illustrates task design and trial timing.

2.3. Oculomotor procedures

The experimental stimuli were projected into the bore of the scanner on a screen that was viewed by the subjects through an angled mirror. Eye movements were recorded in the scanner at 1000 Hz with an infrared video-graphic camera equipped with a telephoto lens (Eyelink, SR Research). The camera focused on the right eye viewed from the flat surface mirror attached inside the radio frequency coil. Trials in which subjects did not hold fixation

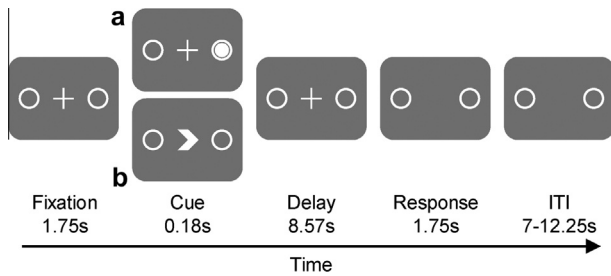


Fig. 1. Stimulus timing and task design schematic. Note: The figure illustrates the timing and task design of the two saccade task conditions. Stimulation of the fixation, delay, response and ITI period was identical for both conditions (a and b). In the visually-guided saccade task (a) the direction of the saccade was indicated by an exogenous cue, a white circle in the target placeholder (Cue). In the simple internally-guided saccade task (b) the direction of the upcoming saccade was indicated by an endogenous arrow-like symbol pointing towards the left or right placeholder (Cue). ITI, inter-trial interval.

during the fixation period at the beginning of the trial were discarded. Nine-point calibrations were performed at the beginning of each session and between blocks if necessary. Eye movement data were transformed into degrees of visual angle, calibrated using a third order polynomial algorithm that fit eye positions to known spatial positions and scored off-line with in-house software. In total, 15.78% of all trials from all subjects were discarded from analyses due to technical difficulties while recording or non-compliance (e.g., uninstructed saccades, anticipatory saccades, missed saccades). Only trials in which the first saccade landed on the correct target (left or right placeholder) and remained there until the fixation cross reappeared were further analyzed. Saccade onsets were defined by the velocity of the eye movement reaching 30 m/s. Saccadic reaction times were computed by semiautomatic routines. The data were also inspected visually, trial by trial, and corrections were made if necessary.

2.4. Neuroimaging methods

Functional magnetic resonance imaging (fMRI) at 3 T (Allegra, Siemens) was used to measure blood oxygenation level dependent (BOLD) changes in cortical activity. Images were acquired using custom radio-frequency coils (NM-011 transmit head coil and NMSC-021 four-channel phased array receive coil; NOVA Medical, Wakefield, MA) placed over lateral frontal and parietal cortices. During each fMRI scan, a time series of volumes was acquired using a T2⁺-sensitive echo planar imaging pulse sequence (repetition time 1.750 ms, echo time 30 ms, flip angle 80°, 32 slices; 3 mm³ isotropic voxels, inplane field of view 192 mm², bandwidth 2112). To minimize head motion we stabilized subjects with foam padding around the head.

2.5. fMRI data preprocessing and surface-based statistical analysis

To correct for residual head motion we used image registration (MCFLIRT; motion correction using the linear image registration tool from Oxford University's Center for Functional MRI of the Brain; Jenkinson, Bannister, Brady, & Smith, 2002). Time series of each voxel were band-pass filtered (0.027–0.29 Hz) to compensate for the slow drift that is typically seen in fMRI measurements. The time series of each voxel were divided by its mean intensity resulting in percent signal modulation thereby compensating for the decrease in mean image intensity with distance from the receive coil. Finally, the data was spatially smoothed to 8 mm at full-width half maximum.

For both delayed saccade tasks, each within-trial event (that is, cue, delay and response) was modeled separately and all independent variable regressors were entered into a modified general linear model for statistical analysis using VoxBo ([\[bo.org\]\(http://www.voxbo.org\)\). The first-order polynomial \(that is, ramp\) was used to estimate delay period activity at the group level for two reasons: First, it significantly predicted delay period activity at the individual subject level. Second, it progressively emphasizes the later portion of the delay, thereby decontaminating it from cue related activity.](http://www.vox-</p>
</div>
<div data-bbox=)

We used Caret (Van Essen et al., 2001, <http://www.nitrc.org/projects/caret/>) for anatomical segmentation, gray-white matter surface generation, flattening and multi-fiducial deformation mapping to the population-averaged landmark- and surface-based atlas for each subject. Compared to standard volumetric-normalization methods a surface space that applies precise anatomical landmark constraints (e.g. central sulcus, sylvian and calcarine fissures) for registration provides greater spatial precision (Van Essen, 2005).

Single subject statistical maps based on beta weights were created for each contrast of interest and then deformed into the same atlas space. Within spherical atlas space, *t* statistics were computed for each contrast of interest across subjects. A nonparametric statistical approach based on permutation tests integrated in Caret software was used to address the problem of multiple statistical comparisons (Van Essen et al., 2001). First, for each contrast of interest a permuted distribution of clusters of neighboring surface was constructed. To this end, the signs of the beta values for each node were randomly permuted for each subject's surface. Then the maps of all subjects of the respective contrast were subjected to a one sample *t*-test. This procedure was performed in 1000 iterations, *N*, to compute a permutation distribution. Second, from this distribution, only clusters with neighboring surface nodes with *t*-values >3.0, corresponding to an uncorrected *p* value of .005 (*df* = 12) were chosen. This cutoff allowed intense focal clusters of activity to pass while not losing diffuse large clusters of activity. The resulting suprathreshold clusters were ranked by their area. Finally, areas of suprathreshold clusters of *t*-statistics of the experimental data were compared to the areas of the top 5% of the clusters in the permuted distribution. Suprathreshold clusters with areas greater than the critical suprathreshold cluster size, $C = N\alpha + 1$ were considered significant with corrected *p* values at $\alpha = 0.05$.

2.6. Region of interest (ROI) time-series procedures

To analyze the time course of BOLD signal change, regions of interest (ROIs) were defined for the sPCS and IPS in both hemispheres. ROIs were obtained by tracing the relevant anatomical area on each participants high-resolution scans. This contained the superior precentral sulcus at its junction with the superior frontal sulcus for the sPCS and the full extent of the IPS. In each of the individual ROIs the 20 voxels with the strongest main effect of the linear combination of both task conditions were selected. Time series of BOLD responses were averaged across voxels in each individual ROI, averaged across subjects from analogous ROIs and plotted time locked to the presentation of the cue until four volumes after the response.

Separate cue, delay and response indices were calculated to quantify and evaluate the time series data. Cue period activation was defined as the average activation of all time points from the presentation of the cue until 5.25 s after the cue, delay period activation was defined as the average activation of all time points from 5.25 s after the cue until 10.5 s after the cue, response period activation was defined as the average activation of all time points from 1.75 s after the response signal until 7 s after the response. An ANOVA for repeated measures (hemisphere × task condition) was conducted to check for hemispheric differences. Since none were detected, data from left and right ROIs were combined. Contralateral activation was defined as activation in the left ROI when the target location of the saccade was to the right and activation in the right ROI when the target location was to the left. Ipsilateral

activation was defined as activation in the left ROI when the target location of the saccade was to the left and activation in the right ROI when the target location was to the right. A laterality index was calculated for each subject to quantify the contrast of contralateral and ipsilateral BOLD activation $[(\text{contralateral} - \text{ipsilateral}) / (\text{contralateral} + \text{ipsilateral})]$. *T*-Tests were calculated on cue, delay and response period activation as well as laterality indices to test specific hypotheses.

2.7. Multi-voxel pattern analysis (MVPA)

We used the Princeton MVPA Toolbox (www.pni.princeton.edu/mvpa) to test the hypothesis that multi-voxel patterns of BOLD response in ROIs (sPCS and IPS) could predict where a saccade was made in the cue, delay and response period (as defined for the ROI analysis in Section 2.6). Incorrect trials were excluded from the analysis, and the time series of each voxel was motion corrected (see Section 2.5) and normalized by subtracting the mean activity and dividing by the standard deviation to yield a mean of 0 and standard deviation of 1. The BOLD epoch used for analysis was shifted by 3.5 s to adjust for the hemodynamic lag.

To evaluate decoding performance, we performed a leave-one-run-out cross-validation procedure. With one run left out for the independent test data, the remaining runs were used for selecting voxels and training a classifier. First, we identified voxels whose activity differed according to saccade direction using ANOVAs (AFNI deconvolution; Cox, 1996) that contrasted saccade direction (i.e., leftward versus rightward saccades) collapsing across task conditions (internally-guided and visually-guided saccades) for each trial period (cue, delay, response). To maintain statistical independence between voxel selection and later classification, we iteratively used only five of the data runs and left out the one run that was going to be used for testing the classifiers performance. Then, we selected 100 voxels from within our ROIs (see Section 2.6) that had the highest *F*-values from the ANOVA. Second, we used logistic regression to train a classifier to predict the direction of the saccade based on the patterns of BOLD activity in the selected voxels. This was done separately for voxels within each ROI and for each trial epoch (cue, delay, response) and separately for each of the two task conditions (visually and internally-guided saccades). Trial epochs were defined as in the times series analysis described above, with each trial period lasting for three TRs, that is the cue period lasting from the presentation of the cue until 3.75 s after the cue, the delay period lasting from 3.75 s after the cue until 7.5 s after the cue and the response period lasting from 1.75 s after the response signal until 5.5 s after the response signal. Third, we tested the decoding performance of the classifier using the trials from the run left out of the voxel selection and training. We repeated this procedure six times until each run of six runs had been used for the test data and the decoding accuracy was averaged across six predictions. Finally, significance was determined by permutation testing where the entire procedure was repeated for sets of data in which the trial labels (i.e., saccade direction) were randomly shuffled 1000 times per iteration (6 runs \times 1000 shuffles = 6000 draws) to create a null distribution. Classifier performance outside of the 95% confidence interval of the null distribution was considered to be significant at the $p < 0.05$ level. For the present data the significance threshold corresponding to $p < 0.05$ determined by this procedure was an accuracy of 58.3%.

3. Results

3.1. Saccade latencies

The percentage of correct trials and anticipatory saccades did not differ between the two tasks (accuracy, $t(12) = -1.92$,

$p = .079$; anticipatory saccades, $t(12) = 1.52$, $p = .077$). Latencies did not differ between the two task conditions (delayed internally-guided saccades, $M = 415.1$ ms, $SD = 56.9$ ms, $t(12) = -1.25$, $p = .118$; delayed visually-guided saccades, $M = 409.6$ ms, $SD = 56.8$ ms). This is not surprising as the subjects had time to prepare their saccades during the long delay periods, which often nullify latency differences (Curtis & Connolly, 2008). Moreover, significant differences in saccade latencies between the groups would have complicated interpreting the BOLD data during the response period (Tark & Curtis, in press).

3.2. Surface-based statistical tests

Fig. 2 shows that within well-known oculomotor areas BOLD activity increased significantly during processing the cue, preparing the saccade during the delay and executing the saccade, across saccade tasks. While subjects encoded the exogenous or the endogenous cue we found bilateral activation in the superior precentral sulcus (sPCS) comprising the sPCS, the lateral precentral sulcus (IPCS), the intraparietal sulcus (IPS), the bridging lobule across the IPS, the posterior part of the middle temporal gyrus (MTG), the lateral occipital sulcus (LOS), the middle occipital gyrus (MOG), and the superior parietal gyrus (SPG). In the right hemisphere, activation in the IPCS was extended further ventral towards the inferior precentral sulcus. Parietal and occipital activation was more extended in the right hemisphere. In the left hemisphere there was additional activation in the lingual gyrus and lingual sulcus. In the delay period when subjects prepared a saccade bilateral activation only persisted in the sPCS and the right IPCS. In the response period when subjects executed the saccade there was bilateral activation in the sPCS, in the IPS, the superior parietal gyrus and the bridging lobule across the IPS, the anterior occipital sulcus at the junction with the inferior temporal sulcus, the middle occipital gyrus (MOG) and the lingual gyrus. Additionally activation was found in the left paracentral gyrus, the right IPCS, the right middle temporal gyrus, the right angular gyrus and the right middle occipital gyrus.

Differences in activation between the two task conditions only occurred in the response period, and outside of the traditional oculomotor network. Fig. 3 shows areas with increased activation during delayed internally-guided saccades compared to delayed visually-guided saccades. For the delayed internally-guided saccade condition activation was higher in the left and right frontopolar gyrus. In the right hemisphere this activation was extended dorsally along the medial part of the superior frontal gyrus and ventrally along the medial wall towards the right subgenual anterior cingulate. Further increased activation was found in the left hemisphere in the angular gyrus, the middle temporal gyrus and the cuneus, the middle frontal gyrus and the posterior cingulate gyrus. Table 1 gives coordinates of peak activations the cue, delay and response period across tasks and peak activations of between task differences in the response period.

3.3. Region of interest (ROI) time-series analysis

Since there were no effects of hemisphere or hemisphere in dependence on tasks in either ROI, data from left and right hemispheres were combined (sPCS: hemisphere: $F(1) = .59$, $p = .46$; hemisphere \times task: $F(1) = 1.43$, $p = .26$; IPS: hemisphere: $F(1) = .46$, $p = .51$; hemisphere \times task: $F(1) = .06$, $p = .81$). Time series in the sPCS and IPS were plotted to test our hypotheses. First, we tested whether activity in both ROIs persisted throughout the trial. Activation in the sPCS persisted above baseline during the cue, delay and response period in both saccade task conditions (delayed internally-guided saccade: cue period,

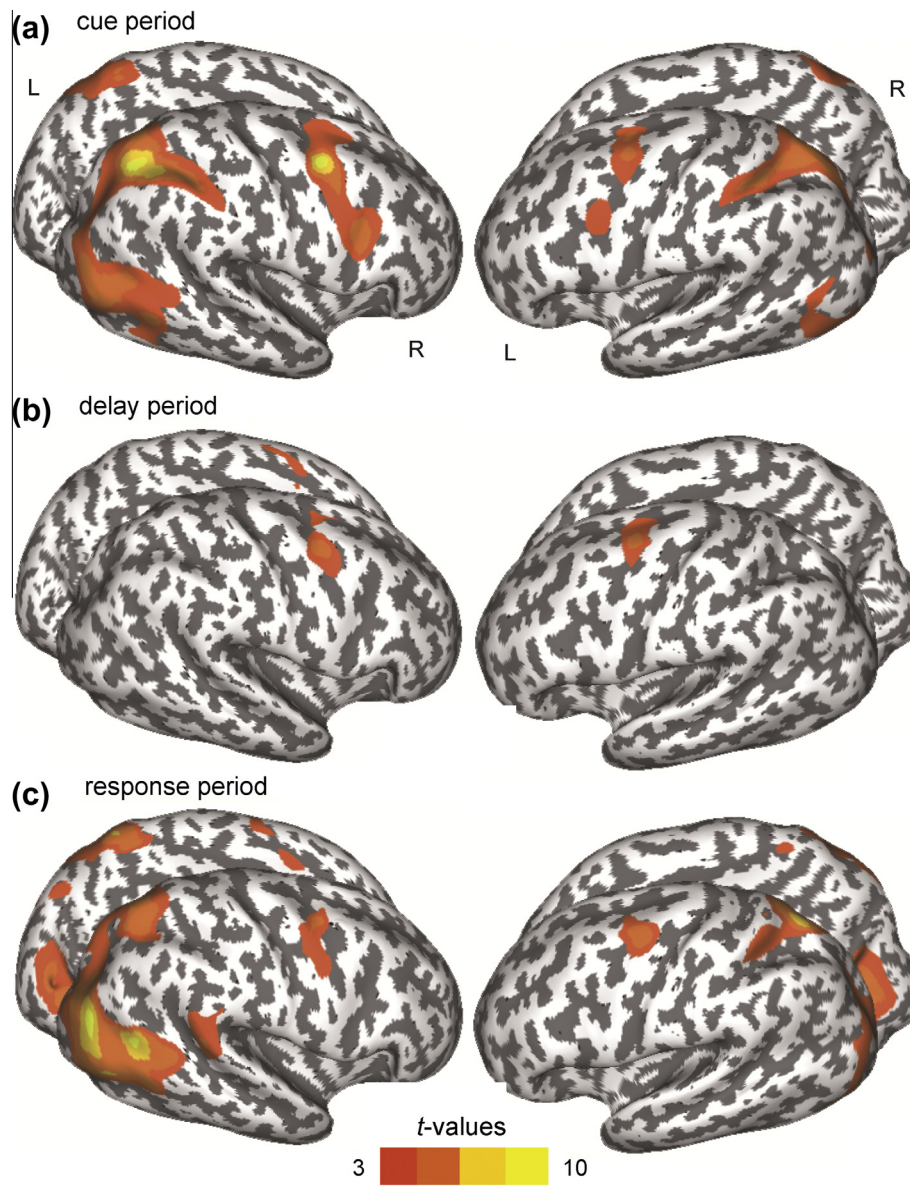


Fig. 2. Surface-based statistical maps of significant BOLD activation for both saccadic task conditions in the cue (a), delay (b) and response period (c). Note: Dark gray color indicates sulci, light gray color indicates gyri; L, left hemisphere; R, right hemisphere; $p_{\text{corrected}} = .05$.

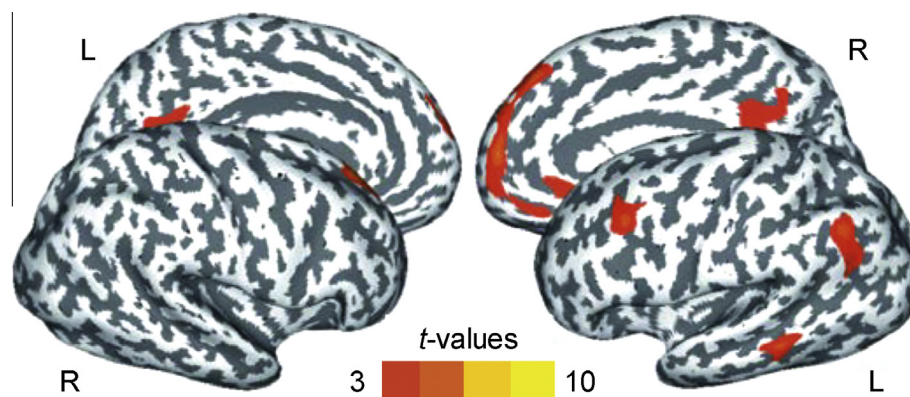


Fig. 3. Surface-based statistical maps of significant BOLD activation that was higher in the delayed internally-guided saccade condition compared to the delayed visually-guided saccade condition in the response period. Note: Dark gray color indicates sulci, light gray color indicates gyri; L, left hemisphere; R, right hemisphere; $p_{\text{corrected}} = .05$.

Table 1
Peak activations in both saccade tasks and peak activations of between task differences.

Anatomical region	Hemisphere	Label	BA	MNI coordinates			T-value
				x	y	z	
<i>Both saccade tasks Cue period</i>							
Intraparietal sulcus	Right	IPS	40	37	-57	42	9.12
Superior precentral sulcus	Right	sPCS	6	33	1	44	9.06
Superior parietal gyrus	Left		7	-26	-66	58	6.30
Lateral precentral sulcus	Right		8	40	12	22	6.14
Middle occipital gyrus	Right		39	49	-78	41	6.14
Middle temporal gyrus	Right		37	54	-63	-7	5.56
Intraparietal sulcus	Left	IPS	40	-36	-46	42	5.38
Superior precentral sulcus	Left	sPCS	6	-32	-5	58	5.30
Superior parietal lobule	Right		7	26	-64	64	5.05
Lateral occipital sulcus	Right		22	41	-58	9	4.71
Lateral precentral sulcus	Left		9	-40	5	35	4.23
Middle occipital gyrus	Left		18	-40	-89	-13	4.05
Lingual sulcus	Left		19	-27	-69	-13	4.05
Inferior occipital sulcus	Left		19	-41	-74	-10	4.01
Lingual gyrus	Left		19	-22	-57	-20	3.83
<i>Delay period</i>							
Superior precentral sulcus	Left	sPCS	6	-30	-5	60	5.89
Superior precentral sulcus	Right	sPCS	6	35	1	44	5.66
Lateral precentral sulcus	Right		6	21	0	52	3.21
<i>Response period</i>							
Middle occipital gyrus	Right		19	48	-77	17	9.23
Lateral occipital sulcus	Right		22	46	-57	11	8.55
Superior parietal gyrus	Left		7	-23	-69	59	7.34
Lingual gyrus	Left		18	-12	-73	-15	6.67
Superior parietal gyrus	Right		7	32	-58	52	6.27
Superior precentral sulcus	Left	sPCS	6	-38	-9	56	6.10
Middle temporal gyrus	Right		37	54	-63	-6	6.00
Superior precentral sulcus	Right	sPCS	6	32	-2	45	5.40
Lateral occipital sulcus	Left		18	-37	-88	-5	4.83
Lingual gyrus	Right		18	3	-73	-7	4.79
Intraparietal sulcus	Right	IPS	40	35	-53	39	4.77
Middle occipital gyrus	Left		19	-26	-92	24	4.54
Intraparietal sulcus	Left	IPS	40	-35	-50	50	4.22
Lateral precentral sulcus	Right		6	47	2	40	4.05
Paracentral gyrus	Left		6	-4	-3	64	3.48
<i>DIGS > DVGS Response period</i>							
Frontopolar gyrus	Right		10	4	57	11	6.31
Superior frontal gyrus	Right		8	21	41	45	5.35
Middle frontal gyrus	Left		9	-47	20	38	4.96
Angular gyrus	Left		39	-53	-62	41	4.91
Middle temporal gyrus	Left		21	-68	-43	-9	4.71
Posterior cingulate gyrus	Left		23	-3	-60	11	4.39
Frontopolar gyrus	Left		31	-6	64	27	3.61
Subgenual anterior cingulate gyrus	Right		24	6	30	-7	3.53

Note: BA, Brodmann area; DIGS, delayed simple internally-guided saccade task; DVGS, delayed visually-guided saccade task. $p_{corrected} = .05$.

$t(12) = 4.26, p = .001$; delay period, $t(12) = 2.50, p = .028$; response period, $t(12) = 5.75, p < .000$; delayed visually-guided saccade: cue period, $t(12) = 5.56, p < .000$; delay period, $t(12) = 3.99, p = .002$; response period, $t(12) = 7.98, p < .000$). In the IPS, BOLD activation was above baseline only in the cue period in both saccade conditions (delayed internally-guided saccade task: cue period, $t(12) = 2.75, p = .018$; delayed visually-guided saccade: cue period, $t(12) = 4.61, p = .001$). Second, we tested whether brain activation within each ROI differed between the two task conditions. BOLD responses during the delayed internally-guided saccade condition did not differ from the delayed visually-guided saccade condition in any trial period in the sPCS and IPS. Third, to evaluate laterality differences a laterality bias index was computed for cue, delay and response period in each ROI. There were no significant differences in laterality between the two task conditions within each ROI or between each ROI within each task condition. Therefore, based on the average BOLD responses within oculomotor ROIs, we could not differentiate between which task the subjects were performing or which direction saccades were directed (see Fig. 4).

3.4. Multivoxel pattern analyses

First, within each trial epoch we computed whether classification performance exceeded the significance threshold of 58.3% accuracy, corresponding to $p < .05$ given by the permutation test (see Section 2.7). In IPS, the classifier significantly predicted saccade direction in both saccade tasks across all three trial epochs (cue, delay, response). In sPCS, classification was slightly below threshold in predicting the saccade direction in the visually-guided saccade task, but only during the cue epoch; the classifier significantly predicted saccade direction in all other epochs for both saccade tasks. Overall, the pattern of neural activation in both ROIs predicted saccade direction in both task conditions across trial periods.

Second, we tested whether classification accuracy within each ROI differed between the two task conditions. Within the sPCS, classification performance was better for delayed internally-guided saccades than for delayed visually-guided saccades during the cue period ($t(12) = 2.68, p = .02$). Classification within the IPS did not differ between the tasks. Third, we tested whether

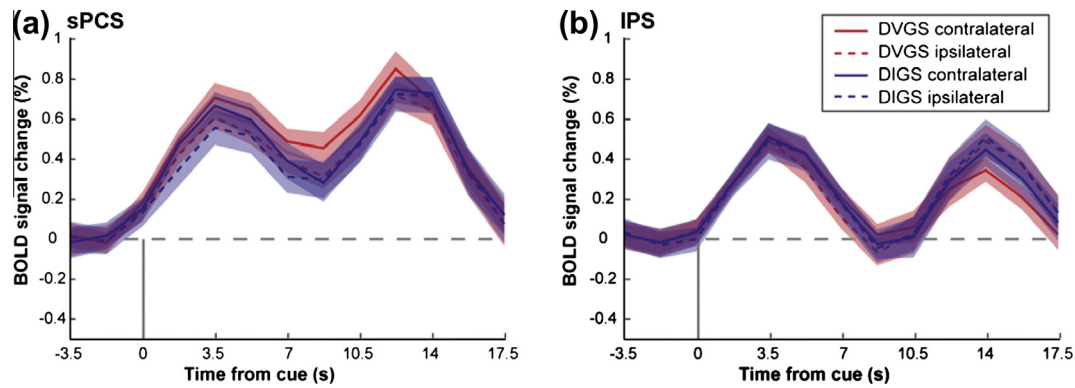


Fig. 4. Group-averaged BOLD time courses time locked to the presentation of the cue in the sPCS and the IPS. Note: (a) The sPCS activity persisted throughout the delay period in the visually-guided saccade and the internally-guided saccade. Activity did not differ between the two task conditions. (b) IPS activity did not persist throughout the delay in both task conditions and activity did not differ between the two conditions. DIGS, delayed internally-guided saccade, DVGS, delayed visually-guided saccade.

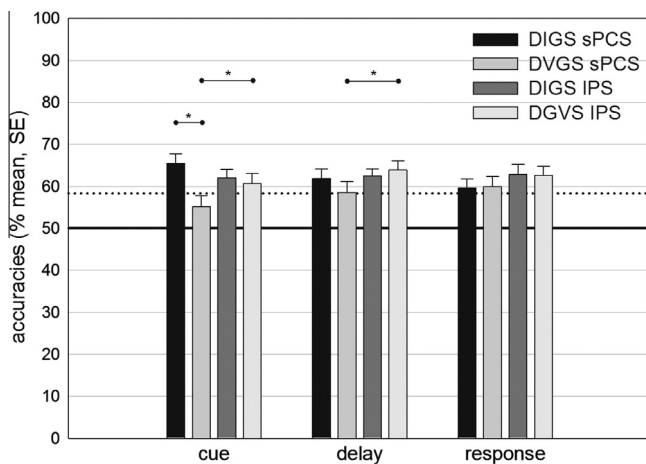


Fig. 5. Classifier accuracy for direction of saccade in the sPCS and IPS for both task conditions in three task periods. Note: sPCS, superior precentral sulcus; IPS, intraparietal sulcus; DIGS, delayed internally-guided saccade, DVGS, delayed visually-guided saccade; cue, 0–5.25 s from cue presentation; delay, 5.25–10.5 s from cue presentation; response, 1.75–7 s from response signal; solid line indicates chance level; dotted line indicates significance threshold of $p = .05$ given by the permutation test.

classification accuracy within each saccade condition differed between the ROIs. For delayed internally-guided saccades there was no difference in classification accuracy between sPCS and IPS in any trial period. For delayed visually-guided saccades, classification accuracy was better within the IPS compared to the sPCS during the cue period ($t(12) = -2.42, p = .032$) and during the delay period ($t(12) = -2.58, p = .024$). Fig. 5 shows classifier accuracies.

4. Discussion

In summary, we find that the pattern but not overall level of activation in the IPS and the sPCS can be used to discriminate the direction of an executed saccade regardless of the degree to which it depended on volitional control. These results support the recent findings of Gallivan, McLean, Smith, and Culham (2011), showing that saccade direction could be predicted in both frontal and parietal cortex following an auditory instruction (Gallivan et al., 2011). Moreover, the multivoxel pattern of activity in sPCS when subjects were encoding the symbolic endogenous cue, but not the exogenous cue, could predict the upcoming direction of the saccade. As

soon as the saccade plan was selected, however, activity in sPCS could predict the saccade direction, regardless of whether the saccade was visually-guided or internally-guided. This pattern was stable in sPCS during the preparation delay and the epoch in which the saccade was generated.

In the IPS, differences in the amount of activity during the visually and internally-guided saccade tasks did not discriminate between saccade directions. However, in all epochs of the two conditions, the pattern of voxel activity in the IPS could predict saccade direction. Regardless of saccade condition, the pattern of IPS activity during the encoding of the cue, the preparation of the saccade and the execution of the saccade could predict saccade direction. Notably, information about saccade direction was present in the pattern of activity, despite that the overall level did not persist above baseline across all trial periods.

The involvement of the sPCS in the performance of complex internally-guided or sometimes called volitional saccades is a consistent finding in human neuroimaging literature (Curtis & D'Esposito, 2003; Grosbras, Laird, & Paus, 2005; McDowell, Dyckman, Austin, & Clementz, 2008). In a study that compared antisaccades with visually-guided saccades, Desouza, Menon, and Everling (2003) reported greater activity in sPCS during antisaccades. Since this activation was even found during encoding the instructive cue, the authors concluded that the increased activation reflected mechanisms related to preparatory set (Desouza et al., 2003). This interpretation is in line with lesion studies reporting that unilateral damage to the sPCS cause chronic impaired volitional saccades, but not simple visually-guided saccades (Dias & Segraves, 1999; Rivaud, Muri, Gaymard, Vermersch, & Pierrot-Deseilligny, 1994). The simplification of the volitional saccade task in the current study, as compared to the Desouza et al. (2003) study, may explain why we find no differences in the overall amplitude of sPCS activation. Indeed, the only difference between our two conditions was in the nature of the cue (exogenous vs. endogenous). Studies applying similar paradigms as the present study so far have reported inconsistent results, indicating a subtle effect on BOLD amplitude that can only be detected under certain conditions (Mort et al., 2003; Reuter et al., 2010; Schraa-Tam et al., 2009). However, in the present study the voxel pattern of activity within the sPCS could predict the direction of the forthcoming saccade only when the cue was endogenous or when volitional processes are taxed; the pattern of sPCS activity during the exogenous saccade cue could not predict saccade direction. The patterns of IPS activity during both exogenous and endogenous cues were predictive of the forthcoming saccade direction. These findings support the notion that the frontal cortex, relative to the parietal cortex, provides computations based on internal, goal-directed actions, compared to

external, perceptual-directed actions (Curtis & Connolly, 2008; Curtis & D'Esposito, 2006; Curtis, Rao, & D'Esposito, 2004; Desouza et al., 2003; McDowell et al., 2005). It has to be noted that we cannot rule out the possibility that pattern classification in the sPCS during visually-guided saccades was not significant due to a lack of power in the data. Trial numbers for training were relatively low, though not uncommon in the field (Han, Berg, Oh, Samaras, & Leung, 2013; Kaplan & Meyer, 2012; Nee & Brown, 2012). However, since the number of valid trials did not differ significantly between the two tasks it is at least unlikely that the differential classification results can be explained by differences in statistical power.

The design of the present study did not allow the dissociation of allocation of attention and motor preparation since the location indicated by the instructional cue was identical to the saccade target location. Therefore, the specific pattern for the cue in the internally-guided saccade might also be related to covert orienting in response to the stimulus (Corbetta et al., 1998; Juan, Shorter-Jacobi, & Schall, 2004; Nobre, Gitelman, Dias, & Mesulam, 2000; Tark & Curtis, 2009).

The IPS is considered the human homologue of the lateral intraparietal area in monkeys also known as the parietal eye field (Andersen, Brotchie, & Mazzoni, 1992; Grefkes & Fink, 2005). Studies in humans have shown an involvement of the region in the triggering of saccades and the processing of visuospatial information (Brown, Goltz, Vilis, Ford, & Everling, 2006; Ettinger et al., 2008; Gaymard, François, Ploner, Condy, & Rivaud-Pechoux, 2003; Grosbras et al., 2005; Kapoula, Isotalo, Muri, Bucci, & Rivaud-Pechoux, 2001; Pierrot-Deseilligny, Rivaud, Gaymard, & Agid, 1991). Single cell recordings in monkey LIP neurons and human imaging studies have shown that the area codes the metric of the upcoming saccade in an ocular delayed response paradigm (Mazzoni et al., 1996). The present findings that IPS showed specific patterns of BOLD activation for saccade directions in both task conditions in all trial periods provide further evidence for this account. Since we did not find sustained activation during the delay and the response period but still could predict saccade direction during these trial periods our results indicate that the information coding saccade direction is stored in the spatial distribution of neural activation rather than in the enhanced activation of certain neurons. This interpretation is in line with the finding that the IPS is organized in topographical maps of the contralateral field (Jerde, Merriam, Rigall, Hedges, & Curtis, 2012; Schluppeck, Curtis, Glimcher, & Heeger, 2006). The lack of sustained activity in the IPS is not consistent with other reports on visual working memory tasks (Curtis & D'Esposito, 2006; Schluppeck et al., 2006; Srimal & Curtis, 2008). However, our finding of specific patterns of activation in the absence of sustained activation might explain why sustained activation in the IPS during a visual working memory task has not always been replicated (Offen, Gardner, Schluppeck, & Heeger, 2010).

Notably, the MVPA revealed differences between the two task conditions in the cue period. The cue period reflected processing of the instructive cues. Studies in which visually-guided saccades and volitional saccades have been compared have consistently reported prolonged latencies for volitional saccades (Mort et al., 2003; Reuter et al., 2010). The differences in activation patterns in the cue period we found might reflect processes that lead to these reaction time differences, when the saccade has to be executed right after the cue. However, in the present study latencies did not differ between the internally-guided and the visually-guided saccade condition. This is not unusual in ocular delayed response paradigms, since a delay puts the performance under more cognitive control, thereby gradually increasing the usually shorter latencies of visually-guided saccades (Hutton, 2008). Our results suggest that latency differences between the tasks are related to early processing of the cue. These differences in processing seem

to dissolve during the delay as both saccades are subjected to cognitive control, resulting in similar latencies.

Interestingly, although we only expected to find subtle task condition differences in the brain activation in the classic GLM analysis, there was relatively increased activation for the volitional saccade task condition during the response period in frontal, parietal, temporal and occipital areas. It has been reported that the frontopolar cortex, especially the most anterior regions, is involved in cognitive branching and multitasking behavior, e.g. when subjects postpone the execution of one task to perform another first (Koechlin & Hyafil, 2007). Since subjects had to postpone the execution of the saccade during the delay and had to maintain attention towards the saccadic target it seems coherent that frontopolar regions were involved during the task. However, the multitasking demands were equal in both task conditions, therefore they cannot account for the task differences we found.

In the present study, we found increased activity associated with volitional saccade generation in an area in the left MFG extending towards the left inferior frontal sulcus. A similar area in the MFG has been reported in a study from Curtis, Rao, and D'Esposito (2004) showing increased activation during the delay of an ocular motor delayed response task when the metric of the upcoming saccade was unknown, compared to the metric of the saccade being indicated by a target cue (Curtis et al., 2004). This suggests that this area may be involved in controlling eye movements when there is no direct external reference of the target location.

In summary, our findings demonstrate that it is possible to discriminate the direction of planned saccades that have been cued by exogenous and endogenous cues. MVPA revealed that the spatial pattern of activity in the putative human FEF differs when encoding exogenous and endogenous cues for saccade direction, which was not detected by conventional analyses. Our data provide further evidence on the differences in the frontal and parietal cortex in the control of volitional actions.

Acknowledgments

We thank K. Sanzenbach for technical support. This work was funded by grants of the US National Institutes of Health to C.E.C (EY016407) and by a Ph.D. scholarship of the Stiftung der Deutschen Wirtschaft, Berlin, Germany to J.B.

References

- Andersen, R. A., Brotchie, P. R., & Mazzoni, P. (1992). Evidence for the lateral intraparietal area as the parietal eye field. *Current Opinion in Neurobiology*, 2(6), 840–846.
- Brown, M. R. G., Goltz, H. C., Vilis, T., Ford, K. A., & Everling, S. (2006). Inhibition and generation of saccades: Rapid event-related fMRI of prosaccades, antisaccades and nogo trials. *Neuroimage*, 33(2), 644–659.
- Corbetta, M., Akbudak, E., Conturo, T. E., Snyder, A. Z., Ollinger, J. M., Drury, H. A., et al. (1998). A common network of functional areas for attention and eye movements. *Neuron*, 21(4), 761–773.
- Cox, R. W. (1996). AFNI: software for analysis and visualization of functional magnetic resonance neuroimages. *Computers and Biomedical Research*, 29(3), 162–173.
- Curtis, C. E., & Connolly, J. D. (2008). Saccade preparation signals in the human frontal and parietal cortices. *Journal of Neurophysiology*, 99(1), 133–145.
- Curtis, C. E., & D'Esposito, M. (2003). Persistent activity in the prefrontal cortex during working memory. *Trends in Cognitive Sciences*, 7(9), 415–423.
- Curtis, C. E., & D'Esposito, M. (2006). Selection and maintenance of saccade goals in the human frontal eye fields. *Journal of Neurophysiology*, 95(6), 3923–3927.
- Curtis, C. E., Rao, V. Y., & D'Esposito, M. (2004). Maintenance of spatial and motor codes during oculomotor delayed response tasks. *Journal of Neuroscience*, 24(16), 3944–3952.
- Desouza, J. F. X., Menon, R. S., & Everling, S. (2003). Preparatory set associated with pro-saccades and anti-saccades in humans investigated with event-related fMRI. *Journal of Neurophysiology*, 89(2), 1016–1023.
- Dias, E. C., & Segraves, M. A. (1999). Muscimol-induced inactivation of monkey frontal eye field: effects on visually and memory-guided saccades. *Journal of Neurophysiology*, 81(5), 2191–2214.

- Ettinger, U., Ffytche, D. H., Kumari, V., Kathmann, N., Reuter, B., Zelaya, F., et al. (2008). Decomposing the neural correlates of antisaccade eye movements using event-related fMRI. *Cerebral Cortex*, *18*(5), 1148–1159.
- Fischer, B., Weber, H., Biscaldi, M., Aiple, F., Otto, P., & Stuhr, V. (1993). Separate populations of visually guided saccades in humans: Reaction times and amplitudes. *Experimental Brain Research*, *92*(3), 528–541.
- Gallivan, J. P., McLean, D. A., Smith, F. W., & Culham, J. C. (2011). Decoding effector-dependent and effector-independent movement intentions from human parieto-frontal brain activity. *Journal of Neuroscience*, *31*(47), 17149–17168.
- Gaymard, B., François, C., Ploner, C. J., Condy, C., & Rivaud-Pechoux, S. (2003). A direct prefrontotectal tract against distractibility in the human brain. *Annals of Neurology*, *53*, 542–545.
- Geier, C. F., Garver, K. E., & Luna, B. (2007). Circuitry underlying temporally extended spatial working memory. *Neuroimage*, *35*(2), 904–915.
- Grefkes, C., & Fink, G. R. (2005). The functional organization of the intraparietal sulcus in humans and monkeys. *Journal of Anatomy*, *207*(1), 3–17.
- Grosbras, M. H., Laird, A. R., & Paus, T. (2005). Cortical regions involved in eye movements, shifts of attention, and gaze perception. *Human Brain Mapping*, *25*, 140–154.
- Hallet, P. E. (1978). Primary and secondary saccades to goals defined by instructions. *Vision Research*, *18*, 1279–1296.
- Han, X., Berg, A. C., Oh, H., Samaras, D., & Leung, H. C. (2013). Multi-voxel pattern analysis of selective representation of visual working memory in ventral temporal and occipital regions. *Neuroimage*, *73C*, 8–15.
- Haynes, J. D., & Rees, G. (2006). Decoding mental states from brain activity in humans. *Nature Reviews Neuroscience*, *7*(7), 523–534.
- Hikosaka, O., & Wurtz, R. H. (1983). Visual and oculomotor functions of monkey substantia nigra pars reticulata. III. Memory-contingent visual and saccade responses. *Journal of Neurophysiology*, *49*(5), 1268–1284.
- Hutton, S. B. (2008). Cognitive control of saccadic eye movements. *Brain and Cognition*, *68*(3), 327–340.
- Hutton, S. B., & Ettinger, U. (2006). The antisaccade task as a research tool in psychopathology: A critical review. *Psychophysiology*, *43*, 302–313.
- Jenkinson, M., Bannister, P., Brady, M., & Smith, S. (2002). Improved optimization for the robust and accurate linear registration and motion correction of brain images. *Neuroimage*, *17*(2), 825–841.
- Jerde, T. A., Merriam, E. P., Riggall, A. C., Hedges, J. H., & Curtis, C. E. (2012). Prioritized maps of space in human frontoparietal cortex. *The Journal of Neuroscience*, *32*(48), 17382–17390.
- Juan, C. H., Shorter-Jacobi, S. M., & Schall, J. D. (2004). Dissociation of spatial attention and saccade preparation. *Proceedings of the National Academy of Science*, *101*(43), 15541–15544.
- Kaplan, J. T., & Meyer, K. (2012). Multivariate pattern analysis reveals common neural patterns across individuals during touch observation. *Neuroimage*, *60*(1), 204–212.
- Kapoula, Z., Isotola, E., Muri, R. M., Bucci, M. P., & Rivaud-Pechoux, S. (2001). Effects of transcranial magnetic stimulation of the posterior parietal cortex on saccades and vergence. *NeuroReport*, *12*(18), 4041–4046.
- Koehlin, E., & Hyafil, A. (2007). Anterior prefrontal function and the limits of human decision-making. *Science*, *318*(5850), 594–598.
- Kriegeskorte, N. (2011). Pattern-information analysis: from stimulus decoding to computational-model testing. *Neuroimage*, *56*(2), 411–421.
- Kriegeskorte, N., & Bandettini, P. (2007). Analyzing for information, not activation, to exploit high-resolution fMRI. *Neuroimage*, *38*(4), 649–662.
- Mazzoni, P., Bracewell, R. M., Barash, S., & Andersen, R. A. (1996). Motor intention activity in the macaque's lateral intraparietal area. I. Dissociation of motor plan from sensory memory. *Journal of Neurophysiology*, *76*(3), 1439–1456.
- McDowell, J. E., Dyckman, K. A., Austin, B. P., & Clementz, B. A. (2008). Neurophysiology and neuroanatomy of reflexive and volitional saccades: Evidence from studies of humans. *Brain and Cognition*, *68*(3), 255–270.
- McDowell, J. E., Kissler, J. M., Berg, P., Dyckman, K. A., Gao, Y., Rockstroh, B., et al. (2005). Electroencephalography/magnetoencephalography study of cortical activities preceding prosaccades and antisaccades. *NeuroReport*, *16*(7), 663–668.
- Mort, D. J., Perry, R. J., Mannan, S. K., Hodgson, T. L., Anderson, E., Quest, R., et al. (2003). Differential cortical activation during voluntary and reflexive saccades in man. *Neuroimage*, *18*, 231–246.
- Munoz, D. P., & Everling, S. (2004). Look away: The anti-saccade task and the voluntary control of eye movement. *Nature Reviews Neuroscience*, *5*(3), 218–228.
- Nee, D. E., & Brown, J. W. (2012). Rostral-caudal gradients of abstraction revealed by multi-variate pattern analysis of working memory. *Neuroimage*, *63*(3), 1285–1294.
- Nobre, A. C., Gitelman, D. R., Dias, E. C., & Mesulam, M. M. (2000). Covert visual spatial orienting and saccades: Overlapping neural systems. *Neuroimage*, *11*(3), 210–216.
- Offen, S., Gardner, J. L., Schluppeck, D., & Heeger, D. J. (2010). Differential roles for frontal eye fields (FEFs) and intraparietal sulcus (IPS) in visual working memory and visual attention. *Journal of Vision*, *10*(11), 28.
- Pereira, F., Mitchell, T., & Botvinick, M. (2009). Machine learning classifiers and fMRI: A tutorial overview. *Neuroimage*, *45*(1 Suppl.), S199–209.
- Pierrot-Deseilligny, C., Rivaud, S., Gaymard, B., & Agid, Y. (1991). Cortical control of reflexive visually-guided saccades. *Brain*, *114*(Pt 3), 1473–1485.
- Reuter, B., & Kathmann, N. (2004). Using saccade tasks as a tool to analyze executive dysfunctions in schizophrenia. *Acta Psychologica*, *115*, 255–269.
- Reuter, B., & Kathmann, N. (2007). Impairments of action control in the context of neuropsychological findings in schizophrenia. *Fortschritte der Neurologie, Psychiatrie und ihrer Grenzgebiete*, *75*(10), 607–616.
- Reuter, B., Kaufmann, C., Bender, J., & Kathmann, N. (2010). Distinct neural correlates for volitional generation and inhibition of saccades. *Journal of Cognitive Neuroscience*, *22*(4), 728–738.
- Rivaud, S., Muri, R. M., Gaymard, B., Vermersch, A. I., & Pierrot-Deseilligny, C. (1994). Eye movement disorders after frontal eye field lesions in humans. *Experimental Brain Research*, *102*(1), 110–120.
- Schluppeck, D., Curtis, C. E., Glimcher, P. W., & Heeger, D. J. (2006). Sustained activity in topographic areas of human posterior parietal cortex during memory-guided saccades. *Journal of Neuroscience*, *26*(19), 5098–5108.
- Schraa-Tam, C. K., van Broekhoven, P., van der Geest, J. N., Frens, M. A., Smits, M., & van der Lugt, A. (2009). Cortical and cerebellar activation induced by reflexive and voluntary saccades. *Experimental Brain Research*, *192*(2), 175–187.
- Srimal, R., & Curtis, C. E. (2008). Persistent neural activity during the maintenance of spatial position in working memory. *Neuroimage*, *39*(1), 455–468.
- Tark, K. J., & Curtis, C. E. (in press). Deciding where to look based on visual, auditory, and semantic information.
- Tark, K. J., & Curtis, C. E. (2009). Persistent neural activity in the human frontal cortex when maintaining space that is off the map. *Nature Neuroscience*, *12*(11), 1463–1468.
- Van Essen, D. C. (2005). A Population-Average, Landmark- and Surface-based (PALS) atlas of human cerebral cortex. *Neuroimage*, *28*(3), 635–662.
- Van Essen, D. C., Drury, H. A., Dickson, J., Harwell, J., Hanlon, D., & Anderson, C. H. (2001). An integrated software suite for surface-based analyses of cerebral cortex. *Journal of the American Medical Informatics Association*, *8*(5), 443–459.
- Walker, R., Walker, D. G., Husain, M., & Kennard, C. (2000). Control of voluntary and reflexive saccades. *Experimental Brain Research*, *130*(4), 540–544.